6102 *Inorg. Chem.* **2010**, *49*, 6102–6109
DOI: 10.1021/ic100692v

Inorganic Chemistry
Article

Synthesis of Coordinatively Unsaturated Mesityliron Thiolate Complexes and Their Reactions with Elemental Sulfur

Takayoshi Hashimoto, Yasuhiro Ohki, and Kazuyuki Tatsumi*

Department of Chemistry, Graduate School of Science, and Research Center for Materials Science, Nagoya University, Furo-cho, Chikusa-ku, Nagoya 464-8602, Japan

Received April 12, 2010

The reactions of Fe_2Mes_4 (**1**; Mes = mesityl) with bulky thiols, namely, HSDmp (Dmp = 2,6-dimesitylphenyl), HSDxp (Dxp = 2,6-dixylylphenyl), and HSBtip [Btip = 2,6-(2,4,6-^{i}Pr$_3$C$_6$H$_2$)$_2$C$_6$H$_3$], provided a series of iron(II) mesityl complexes bearing bulky thiolate ligands. These iron complexes are the thiolate-bridged dinuclear complexes $Fe_2Mes_2(\mu\text{-SAr})(\mu\text{-Mes})$ (**2a**, Ar = Dmp; **2b**, Ar = Dxp), the 1,2-dimethoxyethane (DME) adducts (DME)Fe(SAr)(Mes) (**3a**, Ar = Dmp; **3b**, Ar = Dxp), the mixed-valence $Fe^{I}-Fe^{II}$ dinuclear complexes (Mes)Fe(μ-SAr)(μ-$\overline{\text{SAr}}$)$\overline{\text{Fe}}$ (**4a**, Ar = Dmp; **4b**, Ar = Dxp), and a low-coordinate mononuclear complex (Btip$\overline{\text{S}}$)$\overline{\text{Fe}}$(Mes) (**5**). An $[Fe_8S_7]$ cluster $[Fe_4S_3(SDmp)]_2(\mu\text{-SDmp})_2(\mu\text{-SMes})(\mu_6\text{-S})$ (**6**), the core structure of which is topologically relevant to that of the FeMo-cofactor of nitrogenase, was obtained from the reaction of **3a** or **4a** with S_8. The μ-SMes ligand in **6** is formed via insertion of a sulfur atom into the Fe−C(Mes) bond. The formation of cluster **6** from **3a** or **4a** demonstrates that organoiron complexes are applicable as precursors for iron−sulfur clusters.

Introduction

Synthetic iron−sulfur clusters, which are analogous to the active sites in proteins, have been obtained from homogeneous solutions containing iron precursors and sulfur reagents.[1] The structures and yields of the clusters are sensitive to the reaction conditions, and therefore the choices of iron precursors and solvents are important factors to be considered. Thus far, iron chlorides have been commonly used as iron sources, and polar organic solvents such as CH_3CN and CH_3OH have usually been chosen to dissolve iron chlorides and alkaline metal salts of thiolates.[1,2] While the use of iron chlorides has been useful for providing a variety of iron−sulfur clusters containing $[Fe_2S_2]$, $[Fe_3S_4]$, $[Fe_4S_4]$, and $[Fe_6S_6]$ cores,[2] we and others have developed the synthesis of iron−sulfur clusters in toluene,[3,4] using an iron(II) amide complex, $Fe\{N(SiMe_3)_2\}_2$,[5] as the precursor. This approach led us to discover the $[Fe_8S_7]$ cluster,[3a,e] which reproduces the core of a nitrogenase P-cluster.[6] From the same iron amide complex, we have also synthesized another class of $[Fe_8S_7]$ clusters, $[Fe_4S_3(SDmp)]_2(\mu\text{-SDmp})_2(\mu\text{-STip})(\mu_6\text{-S})$ [**A**; Dmp = 2,6-(mesityl)$_2$C$_6$H$_3$ and Tip = 2,4,6-^{i}Pr$_3$C$_6$H$_2$) and $[Fe_4S_3(SDmp)]_2(\mu\text{-SDmp})_2\{\mu\text{-N}(SiMe_3)_2\}(\mu_6\text{-S})$,[3c] whose core structures are topologically analogous to the FeMo-cofactor[7] of nitrogenase (Chart 1). In this work, we extended our synthetic method to that using an organoiron complex Fe_2Mes_4 (**1**; Mes = 2,4,6-Me$_3$C$_6$H$_2$).[8] The reactions of **1** with bulky thiols gave a series of coordinatively unsaturated mesityliron complexes having thiolate ligands, which were subjected to cluster synthesis by reactions with

*To whom correspondence should be addressed. E-mail: i45100a@nucc.cc.nagoya-u.ac.jp.

(1) (a) Holm, R. H. *Acc. Chem. Res.* **1977**, *10*, 427–434. (b) Beinert, H.; Holm, R. H.; Münck, E. *Science* **1997**, *277*, 653–659. (c) Rao, P. V.; Holm, R. H. *Chem. Rev.* **2004**, *104*, 527–559.

(2) For example, see:(a) Herskovitz, T.; Averill, B. A.; Holm, R. H.; Ibers, J. A.; Phillips, W. D.; Weiher, J. F. *Proc. Natl. Acad. Sci. U.S.A.* **1972**, *69*, 2437–2441. (b) Mayerle, J. J.; Denmark, S. E.; DePamphilis, B. V.; Ibers, J. A.; Holm, R. H. *J. Am. Chem. Soc.* **1975**, *97*, 1032–1045. (c) Hagen, K. S.; Reynolds, J. G.; Holm, R. H. *J. Am. Chem. Soc.* **1981**, *103*, 4054–4063. (d) Hagen, K. S.; Watson, A. D.; Holm, R. H. *J. Am. Chem. Soc.* **1983**, *105*, 3905–3913. (e) Coucouvanis, D.; Kanatzidis, M. G.; Dunham, W. R.; Hagen, W. R. *J. Am. Chem. Soc.* **1984**, *106*, 7988–7989. (f) Strasdeit, H.; Krebs, B.; Henkel, G. *Inorg. Chem.* **1984**, *23*, 1816–1825. (g) Cai, L.; Segal, B. M.; Long, J. R.; Scott, M. J.; Holm, R. H. *J. Am. Chem. Soc.* **1995**, *117*, 8863–8864.

(3) (a) Ohki, Y.; Sunada, Y.; Honda, M.; Katada, M.; Tatsumi, K. *J. Am. Chem. Soc.* **2003**, *125*, 4052–4053. (b) Ohki, Y.; Sunada, Y.; Tatsumi, K. *Chem. Lett.* **2005**, *34*, 172–173. (c) Ohki, Y.; Ikagawa, Y.; Tatsumi, K. *J. Am. Chem. Soc.* **2007**, *129*, 10457–10465. (d) Ohki, Y.; Murata, A.; Imada, M.; Tatsumi, K. *Inorg. Chem.* **2009**, *48*, 4271–4273. (e) Ohki, Y.; Imada, M.; Murata, A.; Sunada, Y.; Ohta, S.; Honda, M.; Sasamori, T.; Tokitoh, N.; Katada, M.; Tatsumi, K. *J. Am. Chem. Soc.* **2009**, *131*, 13168–13178.

(4) Harmjanz, M.; Junghans, C.; Opitz, U.-A.; Bahlmann, B.; Pohl, S. *Z. Naturforsch.* **1996**, *51b*, 1040–1048.

(5) Andersen, R. A.; Faegri, K., Jr.; Green, J. C.; Haaland, A.; Lappert, M. F.; Leung, W.-P.; Rypdal, K. *Inorg. Chem.* **1988**, *27*, 1782–1786.

(6) (a) Peters, J. W.; Stowell, M. H. B.; Soltis, S. M.; Finnegan, M. G.; Johnson, M. K.; Rees, D. C. *Biochemistry* **1997**, *36*, 1181–1187. (b) Mayer, S. M.; Lawson, D. M.; Gormal, C. A.; Roe, S. M.; Smith, B. E. *J. Mol. Biol.* **1999**, *292*, 871–891.

(7) Einsle, O.; Tezcan, F. A.; Andrade, S. L. A.; Schmid, B.; Yoshida, M.; Howard, J. B.; Rees, D. C. *Science* **2002**, *297*, 1696–1700.

(8) (a) Machelett, B. *Z. Chem.* **1976**, *16*, 116. (b) Müller, H.; Seidel, W.; Görls, H. *J. Organomet. Chem.* **1993**, *445*, 133–136. (c) Klose, A.; Solari, E.; Floriani, C.; Chiesi-Villa, A.; Rizzoli, C.; Re, N. *J. Am. Chem. Soc.* **1994**, *116*, 9123–9135.

Published on Web 06/07/2010

Chart 1

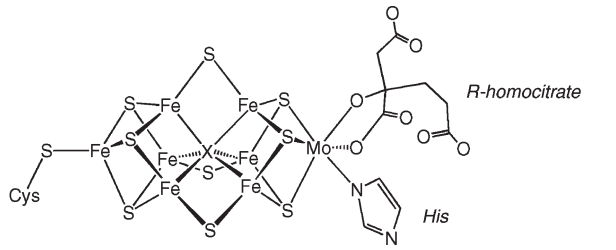

FeMo-cofactor

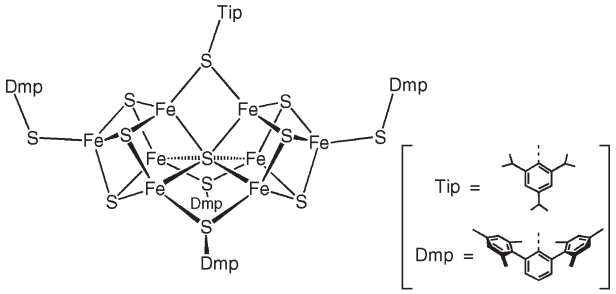

$[Fe_4S_3(SDmp)]_2(\mu\text{-}SDmp)_2(\mu\text{-}STip)(\mu_6\text{-}S)$ (**A**)

elemental sulfur. The insertion of a sulfur atom into the Fe−C(mesityl) bond occurred upon treatment with elemental sulfur, and as a result, an $[Fe_8S_7]$ cluster similar to **A**, $[Fe_4S_3(SDmp)]_2(\mu\text{-}SDmp)_2(\mu\text{-}SMes)(\mu_6\text{-}S)$ (**6**), was obtained.

Results and Discussion

Synthesis of Iron Mesityl Complexes Having Bulky Thiolates. The mesityl group in **1** is susceptible to protonation, and the reaction with $HO(2,4,6\text{-}^tBu_3C_6H_2)$ is known to give the dinuclear mesityl/phenoxide complex $Fe_2Mes(\mu\text{-}Mes)_2\{O(2,4,6\text{-}^tBu_3C_6H_2)\}$.[9] Similarly, protonation of the mesityl group with bulky thiols, namely, HSDmp,[10] HSDxp [Dxp = $2,6\text{-}(xylyl)_2C_6H_3$],[11] and HSBtip [Btip = $2,6\text{-}(2,4,6\text{-}^iPr_3C_6H_2)_2C_6H_3$],[12] took place to provide iron mesityl complexes having bulky thiolate ligands (Scheme 1).

Treatment of an Et_2O solution of **1** with 1 equiv of HSDmp or HSDxp led to the formation of a dark-red solution, from which the thiolate-bridged dinuclear complexes $Fe_2Mes_2(\mu\text{-}SAr)(\mu\text{-}Mes)$ (**2a**, Ar = Dmp; **2b**, Ar = Dxp) were obtained in 72% (**2a**) and 57% (**2b**) yield, respectively. Analogous reactions of **1** with 2 equiv of HSDmp or HSDxp in Et_2O afforded a mixture that contained the dinuclear complexes **2a** or **2b** and the known bis(thiolate) complexes $Fe(SAr)_2$ (Ar = Dmp or Dxp).[10,13] On the other hand, the same reactions in 1,2-dimethoxyethane (DME) gave rise to the monomeric complexes, which were isolated as the DME adducts (DME)Fe(SAr)(Mes) (**3a**, Ar = Dmp; **3b**, Ar = Dxp) in 66% yield for both. While complexes **3a** and **3b** are thermally stable in DME, these complexes dissolved in Et_2O were found to release DME at room temperature to degrade gradually into the mixed-valence Fe^I-Fe^{II} dinuclear complexes (Mes)Fe(μ-SAr)(μ-SAr)Fe (**4a**, Ar = Dmp; **4b**, Ar = Dxp), which were crystallized in 61% (**4a**) and 67% (**4b**) yield, respectively. Consistent with the odd number of d electrons, complexes **4a** and **4b** are EPR-active and show isotropic $S = {}^1/_2$ signals at $g = 2.077$ (**4a**) and 2.079 (**4b**) in toluene at room temperature. These g values are out of the range of organic radicals, indicating that the unpaired spin is metal-centered. The $S = {}^1/_2$ spin state was also supported by their magnetic moments in solution, $\mu_{eff} = 1.86\ \mu_B$ (**4a**) and $1.82\ \mu_B$ (**4b**) at 295 K. Whereas the reaction pathway from **3** to **4** was unclear, bimesityl (Mes−Mes) was formed in 43% yield during the degradation process.

The reaction of **1** with 2 equiv of HSBtip [Btip = $2,6\text{-}(2,4,6\text{-}^iPr_3C_6H_2)_2C_6H_3$] in either Et_2O or DME provided (BtipS)Fe(Mes) (**5**) in 64% yield. In contrast to complexes **3a** and **3b**, the iron center of **5** does not add DME, probably because of the steric hindrance of the SBtip ligand. The bulky Btip group also prevents the formation of sulfur-bridged di- or multinuclear complexes, and indeed most of the precedent SBtip complexes of transition metals are monomeric.[14,15] It is notable that **2a**, **2b**, and **5** are a unique class of heteroleptic and low-coordinate iron complexes,[9,10,13] whereas there have been several low-coordinate, homoleptic iron complexes having amides, thiolates, aryloxides, alkyls, or aryls.[3,8,10,13,14,16]

Structures of Mesityl/Thiolate Complexes. The mesityl/thiolate complexes **2a**, **2b**, **3a**, **3b**, **4a**, **4b**, and **5** were structurally identified based on the crystallographic analysis. The molecular structures of **2a**, **3a**, **5**, and **4a** are shown in Figures 1−4, respectively, with selected bond distances and angles in the captions.

The thiolate ligand and one of the mesityl ligands in **2a** bridge two iron atoms, and both iron atoms are formally three-coordinate (Figure 1). Whereas the SDmp ligand often forms an additional metal−Dmp interaction,[3c,10,13,17] the long Fe−C(Dmp) distances [≥3.3933(14) Å] are indicative of no direct interaction between the Dmp group and iron atoms. The mesityl groups terminally bound to iron are bent from the Fe−Fe axis, with the Fe−Fe−C angles of 152.25(4) and 153.49(4)°. This is probably caused by the steric hindrance between the mesityl groups and the SDmp ligand.

(9) Müller, H.; Seidel, W.; Görls, H. *Z. Anorg. Allg. Chem.* **1996**, *622*, 1968–1974.
(10) Ellison, J. J.; Rhulandt-Senge, K.; Power, P. P. *Angew. Chem., Int. Ed. Engl.* **1994**, *33*, 1178–1180.
(11) Luening, U.; Baumgartner, H. *Synlett* **1993**, *8*, 571–572.
(12) Niemeyer, M.; Power, P. P. *Inorg. Chem.* **1996**, *35*, 7264–7272.
(13) Ohta, S.; Ohki, Y.; Ikagawa, Y.; Suizu, R.; Tatsumi, K. *J. Organomet. Chem.* **2007**, *692*, 4792–4799.
(14) Nguyen, T.; Panda, A.; Olmstead, M. M.; Richards, A. F.; Stender, M.; Brynda, M.; Power, P. P. *J. Am. Chem. Soc.* **2005**, *127*, 8545–8552.
(15) Groysman, S.; Holm, R. H. *Inorg. Chem.* **2009**, *48*, 621–627.
(16) Amide complex:(a) Chen, H.; Bartlett, R. A.; Dias, H. V. R.; Olmstead, M. M.; Power, P. P. *J. Am. Chem. Soc.* **1989**, *111*, 4338–4345. (b) Reiff, W. M.; Schulz, C. E.; Whangbo, M.-H.; Seo, J. I.; Lee, Y. S.; Potratz, G. R.; Spicer, C. W.; Girolami, G. S. *J. Am. Chem. Soc.* **2009**, *131*, 404–405. Thiolate complex:(c) Hauptmann, R.; Kliβ, R.; Schneider, J.; Henkel, G. *Z. Anorg. Allg. Chem.* **1998**, *624*, 1927–1936.Aryloxide complex:(d) Bartlett, R. A.; Ellison, J. J.; Power, P. P.; Shoner, S. C. *Inorg. Chem.* **1991**, *30*, 2888–2894.Alkyl or aryl complex:(e) Müller, H.; Seidel, W.; Görls, H. *Angew. Chem., Int. Ed. Engl.* **1995**, *34*, 325–327. (f) Wehmschulte, R. J.; Power, P. P. *Organometallics* **1995**, *14*, 3264–3267. (g) Viefhaus, T.; Schwarz, W.; Hübler, K.; Locke, K.; Weidlein, J. *Z. Anorg. Allg. Chem.* **2001**, *627*, 715–725. (h) LaPointe, A. M. *Inorg. Chim. Acta* **2003**, *345*, 359–362. (i) Kays, D. L.; Cowley, A. R. *Chem. Commun.* **2007**, 1053–1055.
(17) (a) Ohki, Y.; Sadohara, H.; Takikawa, Y.; Tatsumi, K. *Angew. Chem., Int. Ed.* **2004**, *43*, 2290–2293. (b) Ohki, Y.; Takikawa, Y.; Sadohara, H.; Kesenheimer, C.; Engendahl, B.; Kapatsina, E.; Tatsumi, K. *Chem. Asian J.* **2008**, *3*, 1625–1635. (c) Ohki, Y.; Sakamoto, M.; Tatsumi, K. *J. Am. Chem. Soc.* **2008**, *130*, 11610–11611. (d) Sakamoto, M.; Ohki, Y.; Tatsumi, K. *Organometallics* **2010**, *29*, 1761–1770. (e) Ohki, Y.; Yasumura, K.; Ando, M.; Shimokata, S.; Tatsumi, K. *Proc. Natl. Acad. Sci. U.S.A.* **2010**, *107*, 3994–3997.

Scheme 1

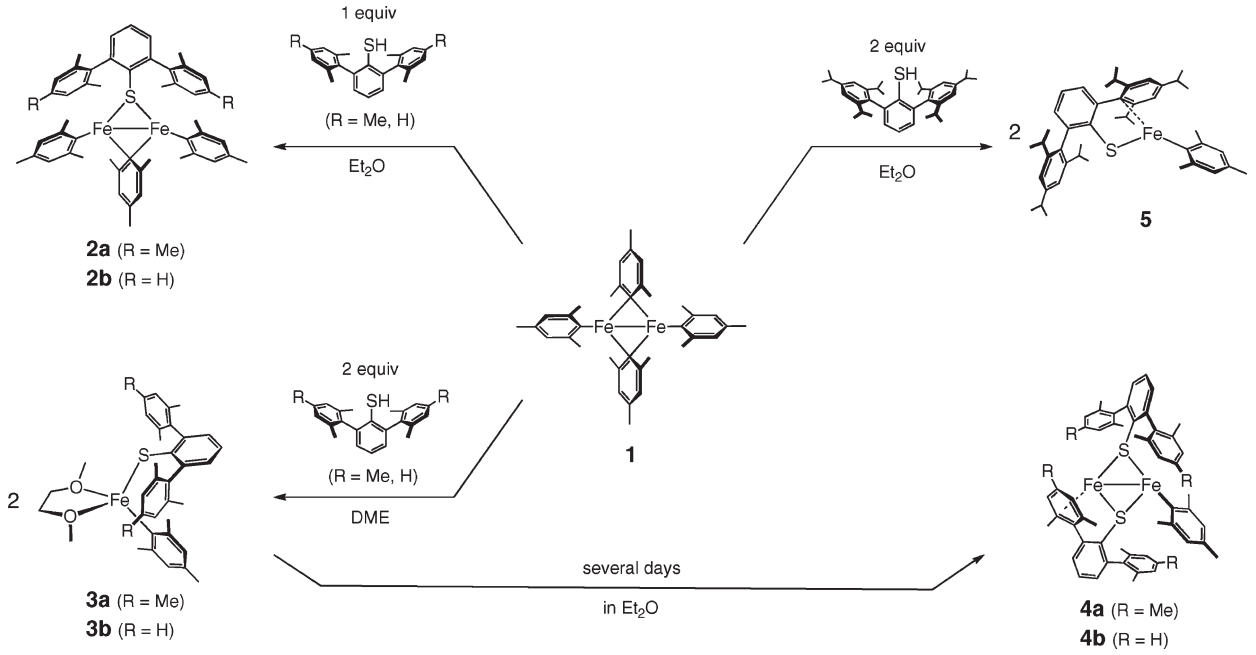

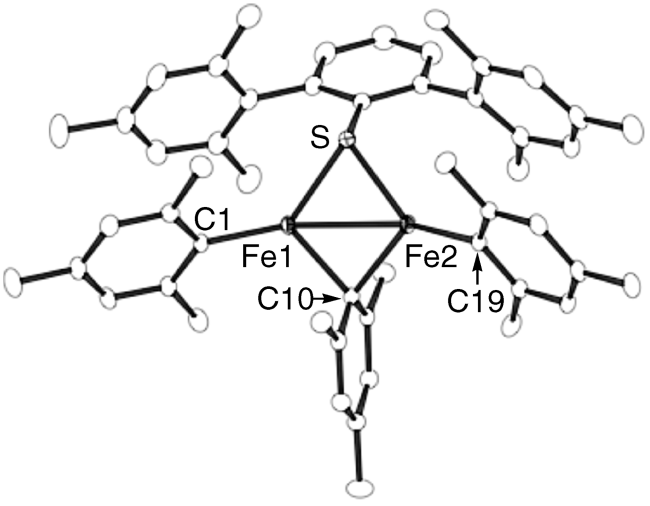

Figure 1. Molecular structure of **2a** with thermal ellipsoids at the 50% probability level. Selected bond distances (Å) and angles (deg): Fe1−Fe2 2.7419(2), Fe1−S 2.3253(4), Fe2−S 2.3340(4), Fe1−C1 2.0195(13), Fe1−C10 2.1139(13), Fe2−C10 2.1243(15), Fe2−C19 2.0135(15); Fe1−S−Fe2 72.098(13), Fe1−C10−Fe2 80.62(5), S−Fe1−C10 103.27(4), S−Fe2−C10 102.65(3), Fe2−Fe1−C1 152.25(4), Fe1−Fe2−C19 153.49(4).

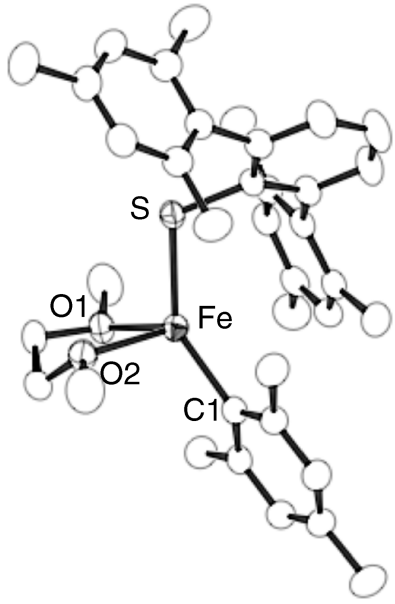

Figure 2. Molecular structure of **3a** with thermal ellipsoids at the 50% probability level. Selected bond distances (Å) and angles (deg): Fe−C1 2.0482(19), Fe−S 2.3218(5), Fe−O1 2.1473(13); S−Fe−C1 142.28(5), S−Fe−O1 98.41(4), C1−Fe−O1 116.64(6), O1−Fe−O2 75.27(4).

It is notable that the iron mesityl groups are nearly parallel to the Dmp mesityl groups, with interplane angles of 3.71(6) and 8.32(6)° and with the shortest ring-to-carbon distances of 3.235(3) and 3.372(3) Å. As indicated by these distances and interplane angles, $\pi-\pi$ interactions probably exist between the iron mesityl and the Dmp mesityl groups. The Fe−Fe distance of 2.7419(2) Å is longer than that of **1** [2.617(1) Å].[8b] One of the possible reasons for the elongation of the Fe−Fe distance is the longer Fe−S(bridge) distances [2.3253(4) and 2.3340(4) Å] in **2a** than the Fe−C(bridge) distances in **1** (2.103−2.105 Å),[8b] while the Fe−S−Fe angle [72.098(13)°] is narrower than the Fe−C−Fe angles of **1** [76.1(2)°] and **2** [80.62(5)°].

The iron center of **3a** is in a distorted tetrahedral geometry (Figure 2), and the S−Fe−C angle [142.28(5)°] is notably larger than the S−Fe−O angles [96.96(4) and 98.41(4)°] and the O−Fe−C angles [104.73(5) and 116.64(6)°]. The large S−Fe−C angle is probably due to the steric congestion between the SDmp and Fe-mesityl groups, and this congestion may also lead to elongation of the Fe−S distance [2.3218(5) Å], which is slightly longer than those of the reported iron(II) complexes having terminal SDmp ligands [Fe−S = 2.2497(6)−2.314(2) Å].[10,13] The distances between the iron atom and the carbon atoms of the SDmp ligand (≥3.5348(16) Å) are too long to form an interaction between the Dmp group and iron. In contrast to **3a**, the iron center of **5** is stabilized with an additional Fe−arene interaction (Figure 3). The Fe−C(arene) distance is 2.432(2) Å, and similar Fe−C(arene)

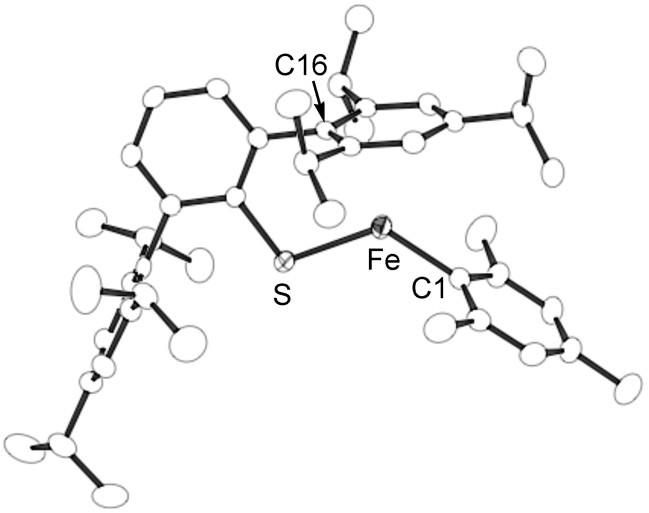

Figure 3. Molecular structure of **5** with thermal ellipsoids at the 50% probability level. Selected bond distances (Å) and angles (deg): Fe−C1 2.038(2), Fe−S 2.2778(7), Fe−C16 2.432(2); C1−Fe−S 125.07(6).

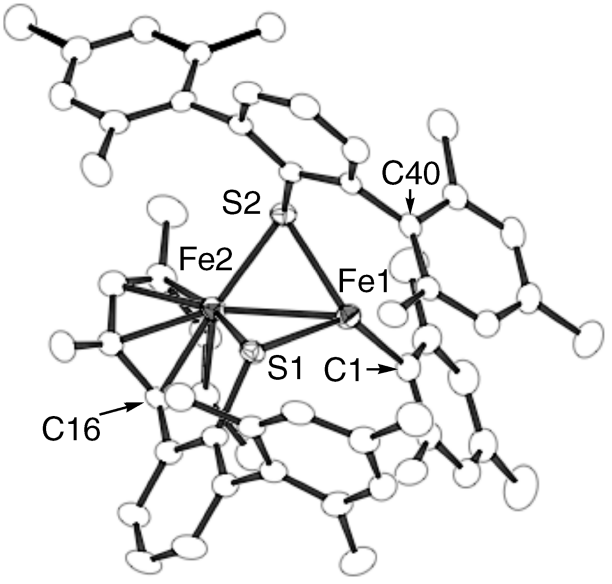

Figure 4. Molecular structure of **4a** with thermal ellipsoids at the 50% probability level. Selected bond distances (Å) and angles (deg): Fe1−Fe2 2.6390(5), Fe1−C1 2.050(2), Fe1−S1 2.4974(6), Fe1−S2 2.3738(8), Fe2−S1 2.2339(8), Fe2−S2 2.2769(6), Fe2−C16 2.041(2), Fe1−C40 2.599(2); S1−Fe1−S2 86.53(2), S1−Fe2−S2 95.53(2), Fe1−S1−Fe2 67.54(2), Fe1−S2−Fe2 69.11(2).

interactions are found in some bulky thiolate complexes of iron such as $Fe(SDmp)_2$ [2.470(3) and 2.535(3) Å],[10] $Fe(SBtip)_2$ [2.427(1) Å],[14] and $Fe(SDmp)\{SC_6H_3\text{-}2,6\text{-}(SiMe_3)_2\}$ [2.389(2) Å].[13] Considering this weak Fe−arene interaction, the iron center in **5** is three-coordinate.

In complex **4a** (Figure 4), both thiolate sulfur atoms are bridging two iron atoms, and one of the thiolate ligands also uses its *o*-mesityl group to cover one of the iron centers (Fe2) as an η^6-arene ligand. The Fe2−C(η^6-arene) distances are 2.041(2)−2.129(2) Å. Such a tethered η^1(S):η^6(arene)-coordination mode for the SDmp ligand is known for some ruthenium complexes.[17b] While the Fe1 atom is formally three-coordinate with two thiolate ligands and a mesityl ligand, one of the Dmp mesityl groups is oriented toward Fe1. The shortest contact between Fe1 and the mesityl

Scheme 2

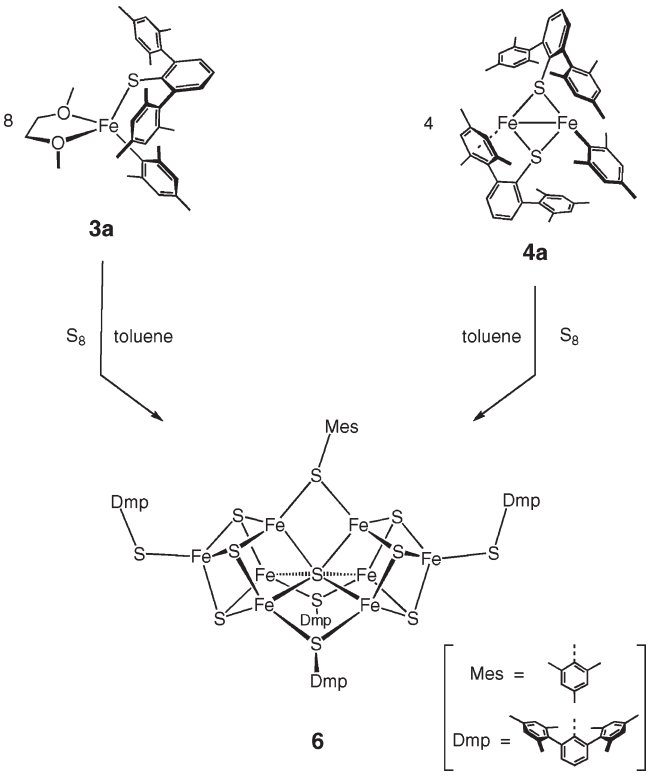

group [Fe1−C40 = 2.599(2) Å] indicates a weak Fe1−mesityl interaction. The Fe−Fe distance [2.6390(5) Å] is shorter than that in **2a** and is indicative of a direct bonding interaction between Fe^{I}−Fe^{II} centers.

Reactions of Mesityliron Thiolate Complexes with S_8. Having a series of mesityl/thiolate complexes of iron, we attempted their reactions with elemental sulfur (S_8) in toluene to synthesize iron−sulfur clusters. These reactions gave black solids after evaporation, and the color was similar to those of iron−sulfur clusters that we had previously reported.[3] However, characterization of the products has been difficult because of the lack of single crystals suitable for X-ray diffraction. After several attempts, an [Fe_8S_7] cluster, $[Fe_4S_3(SDmp)]_2(\mu\text{-}SDmp)_2(\mu\text{-}SMes)(\mu_6\text{-}S)$ (**6**), was found to crystallize from the cyclohexane extracts of **3a** + S_8 or **4a** + S_8 in 17% or 5% yield, respectively (Scheme 2). Whereas some other iron−sulfur complexes may be present in the mother liquor, we have only been successful in crystallizing **6**. It is interesting to note that the μ-SMes ligand in **6** is formed via insertion of a sulfur atom into the iron−mesityl bonds of the precursors. This is a rare example of sulfur atom insertion into an Fe−C σ bond, while analogous sulfur insertion reactions are known for Grignard reagents, alkyl- or aryllithium compounds,[18] and a Cu-Btip complex.[15]

The molecular structure of **6** was determined by crystallographic analysis (Figure 5), and the selected bond distances and angles are listed in Table 1. Two crystallographic mirror planes run through the molecule. One of the planes involves the central sulfur atom (μ_6-S) and the sulfur atoms of the μ-SDmp and μ-SMes ligands. The

(18) Patai, S. *The Chemistry of the Thiol Group, Part 1*; John Wiley & Sons: New York, 1974.

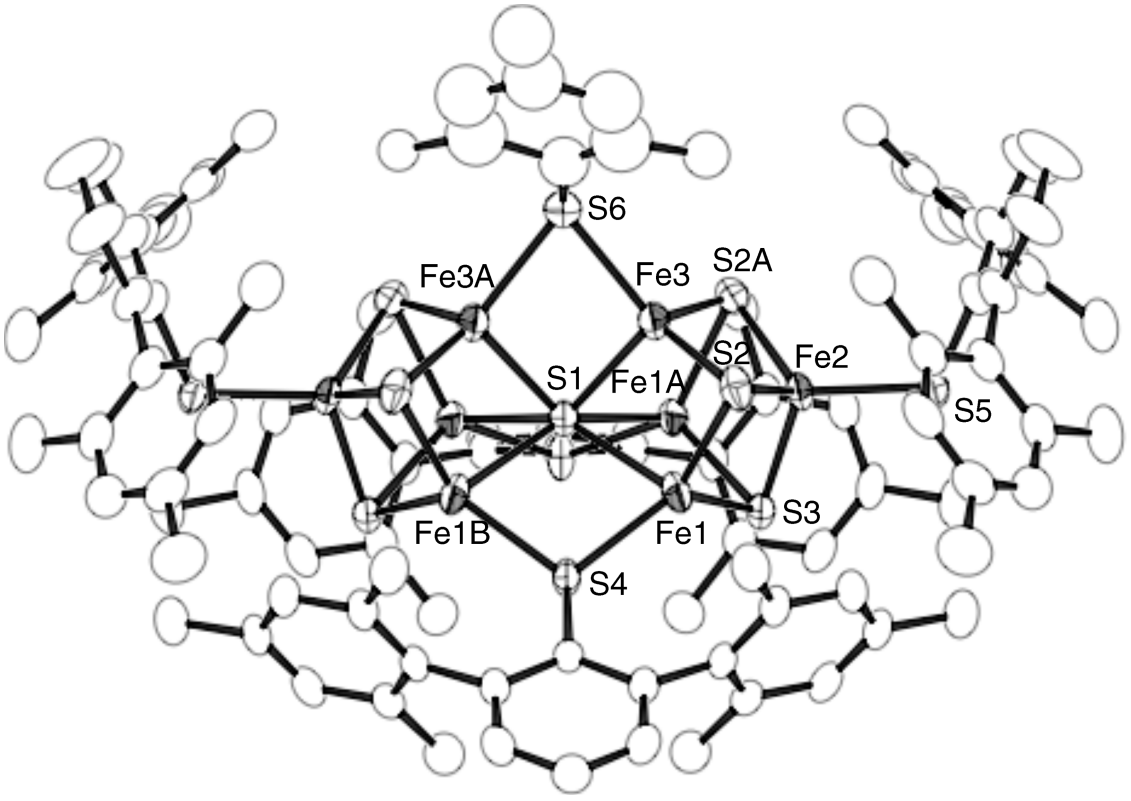

Figure 5. Molecular structure of **6** with thermal ellipsoids at the 50% probability level. Only one of the disordered μ-SMes groups is shown for clarity.

Table 1. Selected Bond Distances (Å) and Angles (deg) for Cluster **6**

Fe1−Fe1A	2.9212(7)	S1−Fe1−S2	99.48(4)	Fe1−S1−Fe1A	73.77(2)
Fe1−Fe1B	3.6506(6)	S1−Fe1−S3	101.84(3)	Fe1−S1−Fe1B	97.18(4)
Fe1−Fe2	2.7626(7)	S1−Fe1−S4	76.81(3)	Fe1−S1−Fe1C	147.72(5)
Fe1−Fe3	2.8527(7)	S2−Fe1−S3	103.41(3)	Fe1−S1−Fe3	74.12(2)
Fe2−Fe3	2.7257(8)	S2−Fe1−S4	135.38(4)	Fe1−S1−Fe3A	134.22(5)
Fe3−Fe3A	2.9714(9)	S3−Fe1−S4	121.00(4)	Fe3−S1−Fe3A	80.69(4)
Fe1−S1	2.4335(9)	S2−Fe2−S2A	104.10(3)	Fe1−S2−Fe2	74.59(2)
Fe1−S2	2.2785(9)	S2−Fe2−S3	104.08(3)	Fe1−S2−Fe3	77.73(3)
Fe1−S3	2.2769(10)	S2−Fe2−S5	117.35(3)	Fe2−S2−Fe3	73.63(3)
Fe1−S4	2.3142(7)	S3−Fe2−S5	108.35(4)	Fe1−S3−Fe1A	79.80(3)
Fe2−S2	2.2810(9)	S1−Fe3−S2	104.09(4)	Fe1−S3−Fe2	75.14(3)
Fe2−S3	2.2537(9)	S1−Fe3−S6	98.33(5)	Fe1−S4−Fe1B	104.12(4)
Fe2−S5	2.2220(12)	S2−Fe3−S2A	105.03(4)	Fe1−S4−C14	122.24(5)
Fe3−S1	2.2956(11)	S2−Fe3−S6	105.38(6)	Fe2−S5−C1	113.94(14)
Fe3−S2	2.2667(10)	S2A−Fe3−S6	136.10(7)	Fe3−S6−Fe3A	77.79(7)
Fe3−S6	2.367(2)			Fe3−S6−C29	112.3(3)

other plane contains the μ_6-S atom, the peripheral iron atoms [denoted as Fe(outer)], and the *ipso*- and *p*-carbon atoms of the central phenyl ring of the SDmp ligand on Fe(outer). The sulfur atom of the μ-SMes ligand is disordered over two positions within the former plane, and the mesityl group is disordered over four positions. For clarity, Figure 5 shows only one of the disordered μ-SMes groups. The core geometry of **6** is almost identical with that of the previously reported **A** (Chart 1),[3c] which has the μ-STip bridge instead of the μ-SMes ligand in **6**. Similarity between **6** and **A** is also found in the Fe−S and Fe−Fe distances, such as Fe(inner)−μ_6S, av. 2.388 Å (**6**) and 2.386 Å (**A**), and Fe(inner)−Fe(outer), av. 2.750 Å (**6**) and 2.759 Å (**A**). Nevertheless, the Fe−SMes distance [2.367(2) Å] and the Fe−Fe distance along with the μ-SMes bridge [2.9714(9) Å] in **6** are slightly longer than the Fe−STip distances [2.3015(12) and 2.3296(11) Å] and the corresponding Fe−Fe distance [2.9103(10) Å] in **A**, while the Fe−μ-SR−Fe angles for these groups are comparable [77.79(7)° (**6**) and 77.87(3)° (**A**)]. These differences may be due to either a steric effect or a packing effect.

The oxidation state of iron centers in **6** is $Fe^{II}_5Fe^{III}_3$ with an odd number of d electrons, and thus **6** is expected to be EPR-active. The EPR spectrum in frozen toluene at 8 K exhibited a rhombic $S = {}^1/_2$ signal at $g = 2.209$, 2.074, and 1.952 (Figure 6, top), the values of which are similar to those for **A** (g = 2.185, 2.068, and 1.957). The $S = {}^1/_2$ ground state for **6** is also supported by the temperature-dependent magnetic susceptibility in the solid state (Figure 6, bottom). The effective magnetic moment at 2 K is 1.84 μ_B, which is close to the spin-only value with one unpaired electron (1.73 μ_B). It is notable that the μ_{eff} value of **6** changes gradually as a function of the temperature, and we have reported an analogous behavior in the magnetic susceptibility of the [Fe_8S_7] model complex of the P-cluster.[3a,e] Whereas elucidation of the

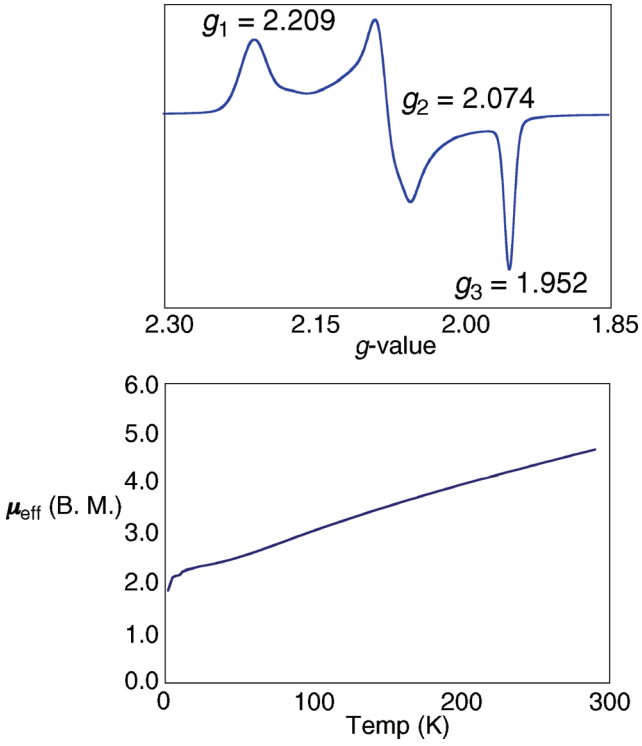

Figure 6. EPR spectrum at 8 K (top) and the temperature-dependent magnetic susceptibility (bottom) of cluster **6**.

spin structure of the $[Fe_8S_7]$ core is difficult because the core is a strongly correlated multispin system, we have previously reproduced the μ_{eff} curve of the $[Fe_8S_7]$ model of the P-cluster, based on the exchange interactions (J values) of magnetic models calculated from the hybrid density functional theory method.[19] An analogous approach could be applied to analyze the spin structure of **6** in future studies.

Concluding Remarks

The iron mesityl complex **1** was found to serve as a precursor for a series of mesityl/thiolate complexes of iron, including a mixed-valence $Fe^{I}-Fe^{II}$ complexes **4a** and **4b** and a low-coordinate heteroleptic complex **5**. The incorporated bulky thiolate ligands, SDmp, SDxp, and SBtip, contribute to the stabilization of the products by steric congestion and by an additional iron−arene interaction in **4a**, **4b**, and **5**.

A new $[Fe_8S_7]$ cluster **6** was obtained from the reactions of **3a** or **4a** with S_8, demonstrating that iron−aryl complexes are applicable as precursors for iron−sulfur clusters. The formation of **6** involves the insertion of a sulfur atom into the Fe−C(Mes) bond. Such an insertion reaction would be used as a synthetic protocol because thiolate ligands constitute important fragments of metal−sulfur clusters. As suggested in the previous study on **A**, cluster **6** possesses the topology of the FeMo-cofactor of nitrogenase (Chart 1 and Scheme 2). The arrangement of iron and sulfur atoms in **6** reveals an analogy with the arrangement of metals and sulfur atoms in the FeMo-cofactor. However, there are substantial differences between these cores, and one of the major the differences is the element of the central atom in **6** (μ_6-S) and the FeMo-cofactor (μ_6-X). Thus, one of the important advances to be made in future studies is encapsulation of X at the center of the metal−sulfur clusters.

Experimental Section

General Procedures. All reactions were carried out using standard Schlenk techniques and a glovebox under a nitrogen or argon atmosphere. Toluene, diethyl ether, tetrahydrofuran, hexane, and 1,2-dimethoxyethane (DME) were purified by the method of Grubbs,[20] where the solvents were passed over columns of activated alumina and a supported copper catalyst supplied by Hansen & Co. Ltd. Solvents, degassed and distilled from sodium benzophenone ketyl, were also used. C_6D_6 and toluene-d_8 were dried by sodium and distilled prior to use. The ^{1}H NMR spectrum was recorded on a JEOL ECA-600. The signals were referenced to the residual proton peak of C_6D_6. UV−vis spectra were measured on a Jasco V560 spectrometer. Elemental analyses were performed on a LECO CHNS-932 microanalyzer, where the samples were sealed into silver capsules in a glovebox. The EPR spectrum was recorded on a Bruker EMX-plus spectrometer at X-band frequencies. X-ray diffraction data were collected on a Rigaku AFC8 or RA-Micro7 equipped with a CCD area detector using graphite-monochromated Mo Kα radiation. The magnetic susceptibility was measured using a Quantum Design MPMS-XL SQUID-type magnetometer, and the crystalline samples were sealed in quartz tubes. Fe_2Mes_4 (**1**),[8c] HSDmp [Dmp = 2,6-(mesityl)$_2$C$_6$H$_3$],[10] HSDxp [Dxp = 2,6-(xylyl)$_2$C$_6$H$_3$],[11] and HSBtip [Btip = 2,6-(2,4,6-^{i}Pr$_3$-C$_6$H$_2$)$_2$C$_6$H$_3$][12] were prepared according to literature procedures.

Synthesis of Fe_2Mes_2(μ-SDmp)(μ-Mes) (2a). An Et_2O (40 mL) solution of HSDmp (380 mg, 1.10 mmol) was added slowly to an Et_2O (20 mL) solution of Fe_2Mes_4 (646 mg, 1.10 mmol) at −80 °C. The mixture was gradually warmed to room temperature and stirred overnight, during which an orange crystalline powder of **2a** appeared. The crystalline powder was collected, washed with hexane, and dried under vacuum (645 mg, 72%). Single crystals suitable for crystallography were obtained from a toluene solution at room temperature. ^{1}H NMR (600 MHz, C_6D_6): δ 38.8 (2H), 33.8 (4H), 30.5 (3H), 25.1 (6H), 24.3 (6H) 13.0 (2H), 8.84 (6H), 5.79 (4H), 1.87 (1H), −6.42 (12H), −11.0 (12H). Anal. Calcd for $C_{51}H_{58}Fe_2S$: C, 75.18; H, 7.18; S, 3.94. Found: C, 75.39; H, 7.08; S, 4.07.

Synthesis of Fe_2Mes_2(μ-SDxp)(μ-Mes) (2b). An Et_2O (30 mL) solution of HSDxp (272 mg, 0.85 mmol) was added slowly to an Et_2O (30 mL) solution of Fe_2Mes_4 (500 mg, 0.85 mmol) at −80 °C. The mixture was gradually warmed to room temperature and stirred overnight. The resulting dark-red solution was evaporated until dryness, and the red residue was extracted with toluene (10 mL). After centrifugation, the extract was evaporated under reduced pressure, and the residue was washed with hexane to afford an orange powder of **2b** (382 mg, 57%). Single crystals suitable for crystallography were obtained from a toluene solution at −40 °C. ^{1}H NMR (600 MHz, C_6D_6): δ 36.2 (2H), 32.8 (4H), 30.2 (3H), 25.3 (6H), 18.2 (6H) 12.6 (2H), 9.98 (2H), 6.24 (4H), 1.07 (1H), −3.54 (12H), −8.42 (12H). Anal. Calcd for $C_{49}H_{54}Fe_2S$: C, 74.81; H, 6.92; S, 4.08. Found: C, 74.80; H, 7.00; S, 3.79.

Synthesis of (DME)Fe(SDmp)(Mes) (3a). A DME (45 mL) solution of HSDmp (577 mg, 0.85 mmol) was added slowly to a DME (30 mL) solution of Fe_2Mes_4 (500 mg, 0.85 mmol) at −50 °C. The resulting dark-yellow solution was evaporated under reduced pressure, and the residue was extracted with Et_2O (30 mL). After centrifugation, the extract was evaporated until dryness. Complex **3a** was isolated as light-yellow crystals (680 mg, 66%) from a mixture of DME (3 mL) and Et_2O (10 mL) at −40 °C. UV−vis (Et_2O): a shoulder was observed at 400 nm.

(19) Shoji, M.; Koizumi, K.; Kitagawa, Y.; Yamanaka, S.; Okumura, M.; Yamaguchi, K.; Ohki, Y.; Sunada, Y.; Honda, M.; Tatsumi, K. *Int. J. Quantum Chem.* **2006**, *106*, 3288–3302.

(20) Pangborn, A. B.; Giardello, M. A.; Grubbs, R. H.; Rosen, R. K.; Timmers, F. J. *Organometallics* **1996**, *15*, 1518–1520.

Table 2. Crystal Data for **2a**−**6**

	2a	**2b**·C_7H_8	**3a**	**3b**·$C_4H_{10}O$
formula	$C_{51}H_{58}Fe_2S$	$C_{56}H_{62}Fe_2S$	$C_{37}H_{46}FeO_2S$	$C_{39}H_{52}FeO_3S$
fw	814.77	878.86	610.68	656.74
temp (°C)	−160	−160	−100	−100
cryst syst	monoclinic	triclinic	monoclinic	triclinic
space group	$P2_1/c$ (No. 14)	$P\bar{1}$ (No. 2)	$P2_1/n$ (No. 14)	$P\bar{1}$ (No. 2)
a (Å)	8.4622(5)	8.8682(8)	12.4774(16)	10.9948(18)
b (Å)	36.244(2)	11.6714(8)	15.7671(19)	11.972(2)
c (Å)	14.4677(9)	24.285(3)	18.322(2)	15.679(2)
α (deg)		77.214(4)		98.720(4)
β (deg)	105.4570(18)	89.527(4)	106.1116(15)	90.870(5)
γ (deg)		71.410(4)		114.882(5)
V (Å^3)	4276.9(4)	2318.1(4)	3462.9(8)	1843.4(5)
Z	4	2	4	2
D_{calcd} (g/cm^3)	1.265	1.259	1.171	1.183
max 2θ (deg)	55.0	55.0	55.0	55.0
no. of data collected	35 673	28 039	26 788	21 803
no. of unique data	9537	10529	7919	8315
no. of variables	545	594	371	398
R1[a]	0.0317	0.0333	0.0429	0.0450
wR2[b]	0.0906	0.0744	0.0810	0.0957
GOF[c]	1.003	1.004	1.002	1.005

	4a	**4b**	**5**	**6**·$(C_6H_{12})_{4.5}$
formula	$C_{57}H_{61}Fe_2S_2$	$C_{53}H_{53}Fe_2S_2$	$C_{45}H_{60}FeS$	$C_{132}H_{165}Fe_8S_{12}$
fw	921.92	865.82	688.88	2583.25
temp (°C)	−100	−100	−100	−100
cryst syst	monoclinic	triclinic	monoclinic	tetragonal
space group	$P2_1/c$ (No. 14)	$P\bar{1}$ (No. 2)	$P2_1/n$ (No. 14)	$P4_2/mnm$ (No. 136)
a (Å)	10.9617(15)	11.436(2)	15.156(2)	24.8871(8)
b (Å)	15.031(2)	11.610(2)	16.5093(19)	
c (Å)	28.612(4)	16.799(3)	17.497(2)	21.4512(9)
α (deg)		96.251(2)		
β (deg)	94.503(2)	99.877(3)	112.8640(15)	
γ (deg)		92.479(3)		
V (Å^3)	4699.7(11)	2180.0(7)	4034.1(9)	13286.2(8)
Z	4	2	4	4
D_{calcd} (g/cm^3)	1.303	1.319	1.134	1.291
max 2θ (deg)	55.0	54.9	55.0	54.9
no. of data collected	37 669	25 679	32 137	104 182
no. of unique data	10589	9886	9174	8036
no. of variables	611	515	477	385
R1[a]	0.0488	0.0339	0.0450	0.0521
wR2[b]	0.0787	0.0673	0.0953	0.1217
GOF[c]	1.001	1.000	1.003	1.007

[a] $R1 = \sum||F_o| - |F_c||/\sum|F_o|$ $[I > 2\sigma(I)]$. [b] $wR2 = [(\sum(w(|F_o| - |F_c|)^2/\sum wF_o^2))^{1/2}$ (all reflections). [c] $GOF = [\sum w(|F_o| - |F_c|)^2/(N_o - N_v)]^{1/2}$ (where N_o = number of observations and N_v = number of variables).

Anal. Calcd for $C_{37}H_{46}FeO_2S$: C, 72.77; H, 7.59; S, 5.25. Found: C, 72.60; H, 7.66; S, 5.38.

Synthesis of (DME)Fe(SDxp)(Mes) (3b). A DME (30 mL) solution of HSDxp (540 mg, 1.70 mmol) was added slowly to a DME (30 mL) solution of Fe_2Mes_4 (500 mg, 0.85 mmol) at −50 °C. The resulting dark-yellow solution was evaporated under reduced pressure, and the residue was extracted with Et_2O (20 mL). After centrifugation, the extract was concentrated to ca. 10 mL under reduced pressure and was stored at −40 °C. Light-yellow crystals of **3b**·$C_4H_{10}O$ were obtained (740 mg, 66%). UV−vis (Et_2O): a shoulder was observed at 400 nm. Anal. Calcd for $C_{35}H_{42}FeO_2S$: C, 72.15; H, 7.27; S, 5.50. Found: C, 72.09; H, 7.15; S, 5.27.

Synthesis of (Mes)Fe(μ-SDmp)(μ-SDmp)Fe (4a). Standing an Et_2O (5 mL) solution of **3a** (28 mg, 0.046 mmol) at room temperature for 1 week resulted in the formation of dark-orange crystals of **4a** (13 mg, 61%), which were collected and dried under vacuum. UV−vis (toluene): λ_{max} = 497 nm (ε = 2200), 621 (ε 980). Evans' method (toluene-d_8, 295 K): 1.86 μ_B. EPR (X-band, microwave 1.0 mW, room temperature): g = 2.077 (isotropic). Anal. Calcd for $C_{57}H_{61}Fe_2S_2$: C, 74.26; H, 6.67; S, 6.96. Found: C, 73.84; H, 6.39; S, 6.75.

Formation of Bimesityl during the Degradation of 3a. Standing an Et_2O (5 mL) solution of **3a** (100 mg, 0.164 mmol) at room temperature for 1 week resulted in the formation of dark-orange crystals of **4a** (34 mg, 45%). The supernatant was treated with aqueous HCl. The organic layer was extracted with Et_2O, and the organic layer was dried over $MgSO_4$. After removal of the solvent under reduced pressure, the residue was extracted with MeOH. The extract was evaporated under reduced pressure to afford a mixture of bimesityl and HSDmp (13 mg). The molar ratio of bimesityl and HSDmp was determined by ^{1}H NMR as 2:3, and the yield of bimesityl was calculated to be 43%.

Synthesis of (Mes)Fe(μ-SDxp)(μ-SDxp)Fe (4b). Standing an Et_2O (3 mL) solution of **3b** (44 mg, 0.076 mmol) at room temperature for 1 week resulted in the formation of dark-orange crystals of **4b** (22 mg, 67%), which were collected and dried under vacuum. UV−vis (toluene): λ_{max} = 489 nm (ε 2100), 616 (ε 990). Evans' method (toluene-d_8, 295 K): 1.82 μ_B. EPR (X-band, microwave 1.0 mW, room temperature): g = 2.079 (isotropic). Anal. Calcd for $C_{53}H_{53}Fe_2S_2$: C, 73.52; H, 6.17; S, 7.41. Found: C, 73.60; H, 6.37; S, 7.53.

Synthesis of (BtipS)Fe(Mes) (5). An Et_2O (40 mL) solution of HSBtp (2.62 g, 5.10 mmol) was slowly added to an Et_2O (30 mL)

solution of Fe_2Mes_4 (1.50 g, 2.55 mmol) at −80 °C. The mixture was gradually warmed to room temperature and stirred overnight. The resulting dark-yellow solution was evaporated under reduced pressure, and the residue was extracted with Et_2O (50 mL). After centrifugation, the extract was evaporated until dryness, and the residue was washed with hexane to afford a yellow powder of **5** (2.26 g, 64%). Single crystals suitable for crystallography were obtained from an Et_2O solution at −40 °C. ^{1}H NMR (600 MHz, C_6D_6): δ 116.1, 113.6, 44.7, 27.8, 4.8, −3.5, −13.3, −53.1. Anal. Calcd for $C_{45}H_{60}FeS$: C, 78.46; H, 8.78; S, 4.66. Found: C, 78.08; H, 8.71; S, 4.55.

Synthesis of [Fe_4S_3(SDmp)]$_2$(μ-SDmp)$_2$(μ-SMes)(μ_6-S) (6). Method A. Complex **3a** (690 mg, 1.13 mmol) and elemental sulfur (S_8; 36 mg, 0.140 mmol) were charged into a Schlenk tube, and toluene (15 mL) was added at 0 °C to dissolve these compounds. After stirring for 5 days at room temperature, the solvent was removed under reduced pressure to give a black oily material. The residue was extracted with hexane (30 mL), and the solution was centrifuged. Evaporation of the extract gave a black powder. The powder was dissolved in cyclohexane (5 mL), and the solution was kept standing at room temperature for several days, affording black crystals of **6**·(C_6H_{12})$_{4.5}$ (63 mg, 17%). UV−vis (toluene, rt): λ_{max} = 450 nm (ε 17000). EPR (X-band, microwave 1.0 mW, 8 K): g = 2.209, 2.074, and 1.952. Anal. Calcd for $C_{132}H_{165}Fe_8S_{12}$: C, 61.37; H, 6.44; S, 14.90. Found: C, 61.44; H, 6.04; S, 15.39.

Method B. Complex **4a** (500 mg, 0.54 mmol) and elemental sulfur (S_8; 35 mg, 0.140 mmol) were dissolved in toluene (15 mL) at 0 °C. After stirring for 5 days at room temperature, the solvent was removed under reduced pressure. An analogous workup, as described in method A, gave black crystals of **6**·(C_6H_{12})$_{4.5}$ (18 mg, 5.1%).

X-ray Crystal Structure Determination. Crystal data and refinement parameters for **2a**−**6** are summarized in Table 2. Single crystals were coated with oil (Immersion Oil type B: Code 1248, Cargille Laboratories, Inc., Cedar Grove, NJ) and mounted on loops. Diffraction data were collected at −100 or −160 °C under a cold nitrogen stream on a Rigaku AFC8 equipped with a Mercury CCD detector or on a Rigaku RA-Micro7 equipped with a Saturn70 CCD detector, using graphite-monochromated Mo Kα radiation (λ = 0.710 690 Å). Six preliminary data frames were measured at 0.5° increments of ω, to assess the crystal quality and preliminary unit cell parameters. The intensity images were also measured at 0.5° intervals of ω. The frame data were integrated using the *CrystalClear* program package, and the data sets were corrected for absorption using the *REQAB* program. The calculations were performed with the *CrystalStructure* program package. All structures were solved by direct methods and refined by full-matrix least squares. Anisotropic refinement was applied to all non-hydrogen atoms except for disordered atoms (refined isotropically), and all hydrogen atoms were put at calculated positions. One isopropyl group of the SBtip ligand in **5** is disordered over two positions in a 1:1 ratio. The SMes bridging ligand of **6** is located at the intersection of two mirror planes, Wycoff position *g*, and is, therefore, 4-hold-disordered. Three crystal solvents (cyclohexane) in **6** are disordered over two or three positions in a 1:1, 2:3, or 3:3:4 ratio, respectively. Additional data are available as Supporting Information.

Acknowledgment. This research was financially supported by Grants-in-Aid for Scientific Research (Grants 18GS0207, 18064009, and 20613004) from the Ministry of Education, Culture, Sports, Science and Technology, Japan. We are grateful to Dr. Rie Suizu and Professors Hirofumi Yoshikawa, Michio Matsushita, and Kunio Awaga (Nagoya University) for aiding us in the SQUID measurements.

Supporting Information Available: X-ray crystallographic data in CIF format for the structures of **2a**−**6**. This material is available free of charge via the Internet at http://pubs.acs.org.